



Boletim de Ciências Geodésicas

ISSN: 1982-2170

Universidade Federal do Paraná

Manfré, Luiz Augusto; Albuquerque, Natália Gallo; Quintanilha, José Alberto
LANDSLIDE HAZARD MAPPING NEAR THE ADMIRAL ÁLVARO
ALBERTO NUCLEAR COMPLEX, RIO DE JANEIRO, BRAZIL.
Boletim de Ciências Geodésicas, vol. 24, no. 1, 2018, January-March, pp. 125-141
Universidade Federal do Paraná

DOI: 10.1590/S1982-21702018000100009

Available in: <http://www.redalyc.org/articulo.oa?id=393956630009>

- How to cite
- Complete issue
- More information about this article
- Journal's webpage in redalyc.org

UABM
redalyc.org

Scientific Information System Redalyc
Network of Scientific Journals from Latin America and the Caribbean, Spain and
Portugal

Project academic non-profit, developed under the open access initiative

LANDSLIDE HAZARD MAPPING NEAR THE ADMIRAL ÁLVARO ALBERTO NUCLEAR COMPLEX, RIO DE JANEIRO, BRAZIL.

Mapeamento do risco de deslizamento associado ao complexo nuclear Almirante Álvaro Alberto, Rio de Janeiro, Brasil

Luiz Augusto Manfré ¹ – ORCID: 0000-0002-1094-1424

Natália Gallo Albuquerque ¹

José Alberto Quintanilha ¹

¹ Universidade de São Paulo, Departamento de Engenharia de Transportes, São Paulo, SP, Brasil.

E-mail: luizmanfre@gmail.com; albuquerque.ng@gmail.com; jaquinta@usp.br

Received in August 9th, 2017.

Accepted in January 16th, 2018.

Abstract:

Technological accidents can be vast in scope and require a rapid response to evacuate the affected region. Access routes to nuclear power stations are essential for the preparation of emergency plans in the event of technological disasters. The Admiral Álvaro Alberto Nuclear Power Plant (Central Nuclear Almirante Álvaro Alberto - CNAAA) in Angra dos Reis, Brazil, is located in a region with high rainfall and rugged terrain. This article presents digital image processing and geoprocessing procedures for mapping landslide-susceptible areas and landslide scars associated with the CNAAA access routes. Digital Elevation Models and their derivations were used to identify landslide-susceptible areas, and LANDSAT images were used to map the land cover. The information was superimposed, and the hazard areas and potential landslide scars were mapped. Most of the study area is medium or high risk for landslide events. Landslides scars mapping achieved over 50% of accuracy representing a potential methodology for the risk assessment and landslides monitoring in the study area. The results demonstrate that further and detailed studies must be performed in the areas in order to maintain the access roads available for eventual evacuations in a technological disaster event.

Keywords: Hazard; Landslides; Technological Accidents; Object Based Image Analysis.

Resumo:

Acidentes tecnológicos podem ter vasta abrangência e necessitam rápida resposta para evacuação da região afetada. As vias de acesso para centrais nucleares são fundamentais para elaboração de planos emergenciais em caso de desastres tecnológicos. Na Central Nuclear Almirante Álvaro Alberto (CNAAA) em Angra dos Reis (RJ), as vias de acesso e sua própria estrutura localizam-se em

How to cite this article: Manfré, L.A. ; et al. Landslide hazard mapping near the Admiral Álvaro Alberto nuclear complex, Rio de Janeiro, Brazil. *Bulletin of Geodetic Sciences*, Vol. 24, issue 1, 125-141, Jan-Mar, 2018.



This content is licensed under a Creative Commons Attribution 4.0 International License.

região com altos índices de precipitação e relevo bastante acidentado. Este artigo visa apresentar procedimentos de processamento digital de imagens e geoprocessamento para o mapeamento de áreas de risco e de cicatrizes de deslizamento associadas às vias de acesso do CNAAA. Modelos Digitais de Elevação e suas derivações foram utilizados para a identificação de áreas de risco, por meio de classificação baseada em objeto. Imagens LANDSAT foram utilizadas para o mapeamento da cobertura do solo. As informações foram sobrepostas e as áreas de risco e as potenciais cicatrizes de deslizamento foram mapeadas. Os resultados apresentam um diagnóstico sobre a susceptibilidade à escorregamentos na área de estudo e das potenciais áreas de risco. As informações apresentadas sobre as áreas associadas às principais vias de acesso evidenciam o risco de ocorrência de escorregamentos que pode afetar a evacuação da região em caso de acidente tecnológico.

Palavras-chave: Risco; Deslizamento; Acidentes Tecnológicos; Classificação baseada em objeto.

1. Introduction

Severe land movements are common in regions with high rainfall and rugged terrain. The construction of highways in these regions can increase the possibility of landslide occurrence (LARSEN & PARKS, 1997; DAI & LEE, 2001; JAISWAL, VAN WESTEN & JETTEN, 2011; PENNA *et al.*, 2013; DI MARTINO *et al.*, 2014). The mapping and identification of hazard areas and landslide scars in regions with highways is important for the prevention and mitigation of severe events (MANCONI *et al.*, 2014). However, mapping and monitoring these events is difficult because highways cross extensive areas, and large quantities of data are required to identify the characteristics and past events (GUZZETTI *et al.*, 2012). The geomorphological characteristics of these regions also make access for *in situ* assessments difficult.

Remote sensing techniques can be used as a viable alternative methodology to detect, monitor and classify landslides (AKSOY & ERCANOGLU, 2012). Several studies have used the diverse data and capabilities of the available satellites and advances in digital image processing technologies to assist in the mapping and prevention of landslides (HSIEH *et al.*, 2014, DONG *et al.*, 2014, ROESSNER *et al.*, 2014).

Several approaches and procedures have been used to predict areas susceptible to landslides; however, this type of forecast is difficult to perform because of the variety and complexity of factors that are related to landslide events, including the lithology, slope form and orientation, slope, drainage network, precipitation, vegetation cover, and anthropic factors, such as the road network, buildings, and deforestation (VIEIRA, 2007).

Many authors have cited the relationships between the slope form, slope, and other geomorphological characteristics with the occurrence of landslides (TAROLLI, SOFIA & FONTANA, 2013; DE VITA *et al.*, 2013; PAULIN *et al.*, 2014). The slope form plays an important role in the distribution of the water content in watersheds, which in turn influences the erosion process and the occurrence of landslides (CRISTOFOLLETTI, 1980). Convex slopes are associated with water dispersion, whereas concave slopes are associated with water accumulation and convergence (SESTINI, 1999) and are therefore the most susceptible to land movements since they are zones

of water flow convergence and contain material that is available for movement (greater quantities of deposited material) (MCKEAN, BUECHE & GAYDOS, 1991, FERNANDES & AMARAL, 1996). The slope is the inclination of the terrain with respect to horizontal, and the mass transport velocity (solid or liquid) is directly related to it (SESTINI, 1999). Thus, the slope and slope form are important data for studies of landslide susceptibility.

Numerous studies have used Digital Elevation Models (DEMs) from remote sensing data to define relief features. Camargo *et al.* (2012) classified relief forms based on different geomorphometric and textural attributes from ASTER/Terra DEM data and obtained a strong correlation between the classification and the reference map. Dragut and Eisank (2012) used Shuttle Radar Topography Mission (SRTM) data and object-based image analysis (OBIA) to classify the topography over the entire Earth's land surface. The authors decomposed the terrestrial surface into homogeneous objects based on elevation data, and the classification criteria were based on the mean elevation values and their respective standard deviations. Their results showed regional scale discontinuity limits. The application of OBIA to a DEM and its derivations allows the segmentation and analysis of several variables in regions of homogeneous relief (EISANK, DRAGUT, BLASCHKE, 2011; DOLEIRE-OLTMANN *et al.*, 2013), which enables the construction of an automated relief classification model based on pre-defined parameters for the area being evaluated (CAMARGO *et al.*, 2012; DRAGUT & EISANK, 2012).

Remote sensing data have also been widely used to assess landslide susceptibility by developing landslide inventory maps (ALEXAKIS *et al.*, 2014). The identification of landslide scars is fundamental to the hazard inventory for understanding the processes that trigger landslides and for interventions in the affected areas (PRADHAN & LEE, 2010).

Several methodologies have been used to identify landslide scars through remote sensing; however, a major problem with this type of mapping in mountainous regions is the acquisition of high-quality data that allow the processing and identification of scars (BARLOW, MARTIN & FRANKLIN, 2003). Aerial photographs, which are commonly used for this type of evaluation (MCKEAN, BUECHEL & GAYDOS, 1991), can accurately identify landslides but have high financial and processing costs and are often unavailable for the most landslide-susceptible areas. Thus, satellite images have emerged as an alternative data source since they can provide a more economical evaluation of large landslide-affected areas and allow the analysis of the region surrounding such landslides, especially in terms of the land cover dynamics (AKSOY & ERCANOGLU, 2012).

Thus, the definition of procedures for mapping hazard areas on a regional scale (1:50,000) using free data and automated procedures that can be incorporated and used by public agencies responsible for monitoring hazard areas is extremely important for natural disaster management associated with important access routes.

The objective of this article is to propose a strategy for mapping hazard areas and identifying landslide scars on a regional scale based on free satellite remote sensing data. The study area is the hydrographic basin in which the Admiral Álvaro Alberto Nuclear Power Plant is located in Angra dos Reis, Rio de Janeiro state (RJ). The study area contains important regional access routes for the power plant, which has the potential for technological accidents.

2. Methodology

2.1 Study area

The study area is the region surrounding the Admiral Álvaro Alberto Nuclear Power Plant (Central Nuclear Almirante Álvaro Alberto - CNAAA) in Angra dos Reis, RJ, southeastern Brazil (Figure 1). The nuclear power plant has two units in operation: Angra 1, which has operated since 1985, and Angra 2, which has operated since 2001 (LOUSADA & FARIAS, 2015). The addition of a third unit, Angra 3, is planned for the future.

The CNAAA is located near Highway BR-101 (a segment of the Rio-Santos Highway), which is the main access route for the area. One of the major risk factors related to the CNAAA and its access routes are natural disasters such as landslides because of the geomorphological, presented in figure 2, and precipitation characteristics (average annual rainfall rate vary from 1,515 mm to 2,200 mm) of the region (ARAÚJO & OLIVEIRA, 1988). The municipality of Angra dos Reis has a history of landslides (PINHEIRO & AGUIAR, 2015), such as the disasters that occurred in December 2002 and January 2010, which were both associated with intense rainfall events that are typical of the tropical rainy season between the months of November and April.

The region is located in the geomorphological domain of the Serra do Mar escarpments, which includes mountainous and rugged terrain. Because the region is covered by unconsolidated material, including talus deposits in the foothills (CPRM, 2007), road cuts make the bases of these escarpments highly unstable and susceptible to landslides.

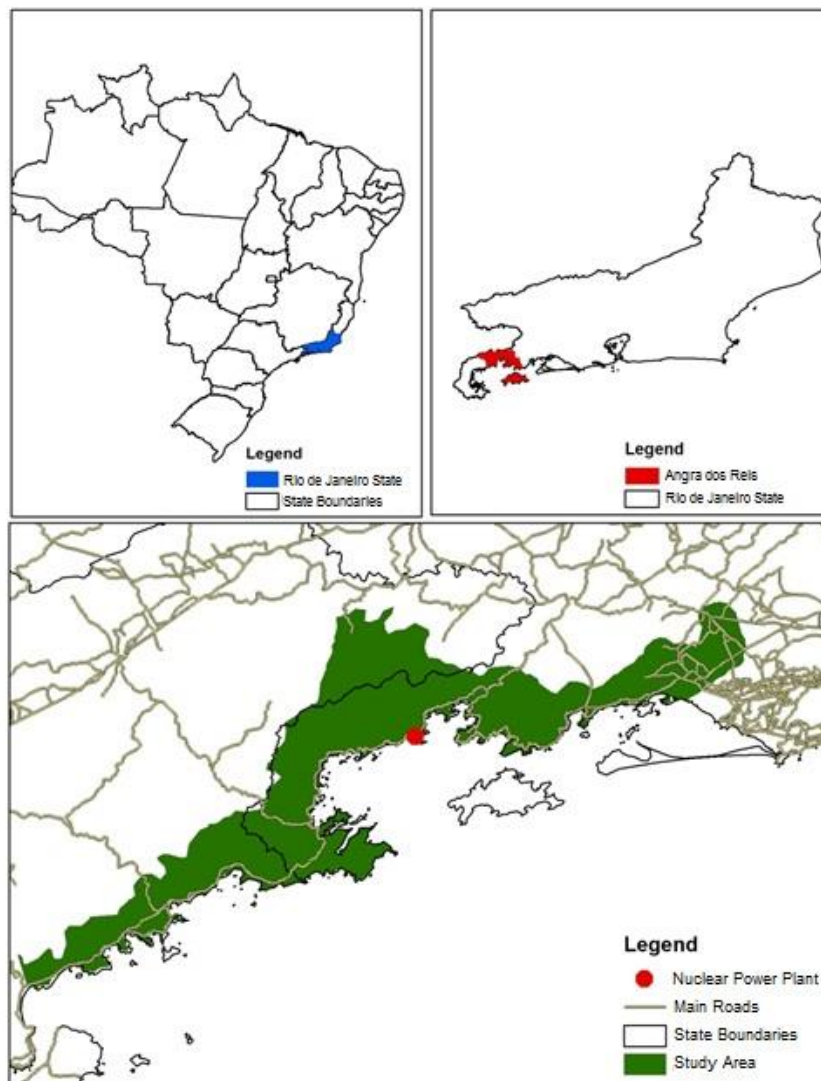


Figure 1: Location of the study area.

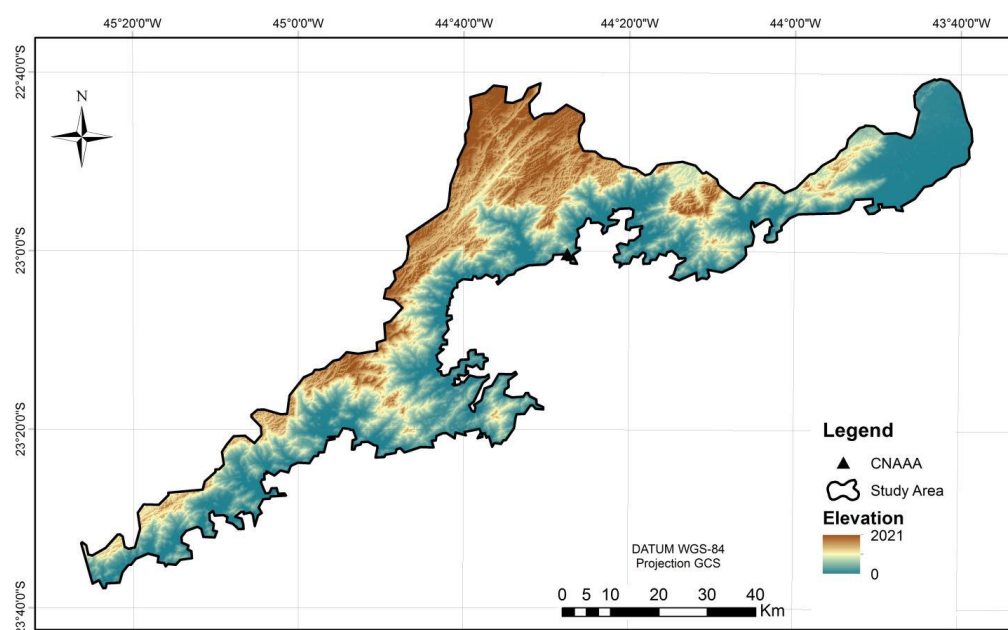


Figure 2: Digital Elevation Model of the study area.

2.2 Digital Image Processing

Freely available TOPODATA and LANDSAT data were used, and digital image processing and geoprocessing techniques were applied to map the landslide-susceptible areas and identify landslide scars associated with the main access roads of the CNAAA. Based on the TOPODATA data, the land relief was classified into three classes of landslide susceptibility: low, medium, and high. The LANDSAT imaging was used to classify the land cover to identify possible landslide scars. The results of the land relief and land cover classifications were analyzed together to provide a preliminary regional assessment and identify areas for additional analysis with more detailed methods.

The landslide-susceptible areas were mapped using the relief classification obtained from the TOPODATA slope and vertical and horizontal slope curvature data. Landslide hazard levels were obtained by applying OBIA to the TOPODATA DEMs with a 30-meter interpolation of the SRTM data of the Brazilian territory (VALERIANO & ROSSETTI, 2012). According to Sestini (1999), this type of information provides the fundamental characteristics for the hazard analysis of a region. The following relief variables were used for the classification process: elevation, slope, drainage density, and horizontal and vertical curvatures.

The Figure 3 flowchart summarizes the relief classification using OBIA. Elevation and Slope data were used for the segmentation step. In this process the objects are defined by areas that presents similar attributes (elevation and slope) in the pixel neighborhood, establishing homogeneous relief areas. The scale and shape parameters of the segmentation process were defined according to the method of Dragut and Eisank (2012), wherein the shape and compactness factors were set to zero, and the scale parameter was defined according to the difference between the local variances of the objects. Thus, a scale parameter of 50 was used, which is similar to the value used in Manfré *et al.* (2014).

The relief classes were defined based on the slope and the vertical and horizontal curvatures. Based on Silva Junior, Silva and Pereira (2016), and IPT (2002), six slope intervals, two classes of vertical curvature, and two classes of horizontal curvature were defined.

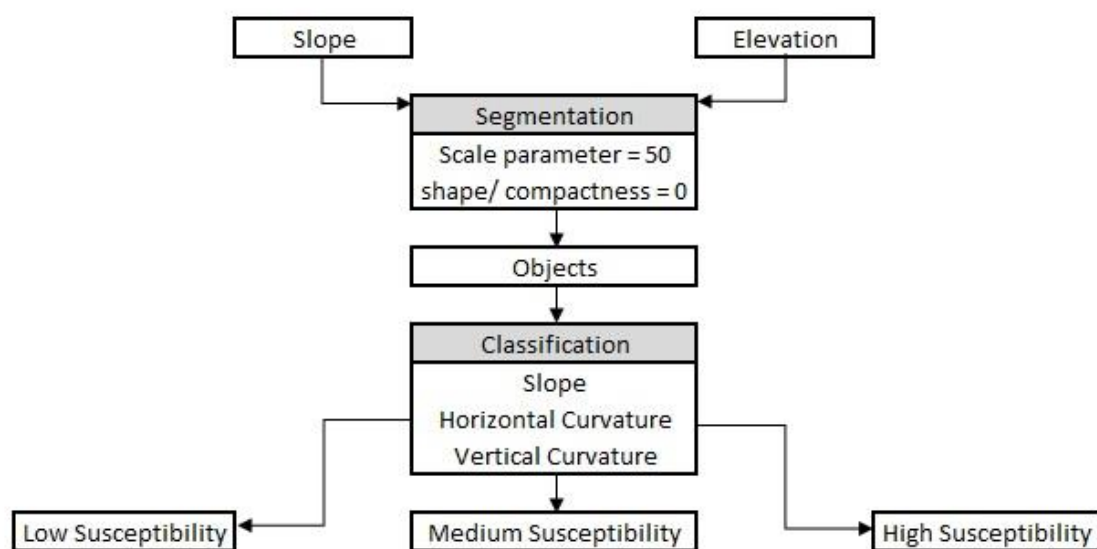


Figure 3. Flowchart of the relief classification process using OBIA.

Table 1 shows the susceptibility classes from the classification described above, which include low, medium, and high. The levels were defined based on theoretical studies (AZEVEDO, 2016; FLORENZANO, 2016; SILVA JUNIOR, SILVA & PEREIRA, 2016; LANGE FILHO, 2016; IPT, 2002 and 1991) that describe the contributions of the slope and the vertical and horizontal curvatures.

Table 1. Landslide susceptibility levels defined based on the combination of classes of slope and of the vertical and horizontal curvatures.

	Slope (degrees)	Vertical concavity	Vertical convexity
Concave Horizontal Curvature	0 to 06	Medium	Low
	06 to 12	Medium	Low
	12 to 20	Medium	Medium
	20 to 30	High	Medium
	30 to 45	High	Medium
	>45	High	High
Convex Horizontal Curvature	0 to 06	Low	Low
	06 to 12	Low	Low
	12 to 20	Medium	Low
	20 to 30	Medium	Low
	30 to 45	Medium	Medium
	>45	High	High

The landslide scars were identified by means of a supervised classification of the land cover in the area of the watershed in question. The land cover classification used two images from the LANDSAT 8 satellite (orbit points 217-076 and 218-076 from August and September 2015, respectively) to cover the entire study area. In order to minimize topographic and radiometric influences on the classification process, the Level-1 Precision and Terrain Corrected Product (L1TP) was used. This product provides radiometric and geodetic accuracy by incorporating ground control points and employs Digital Elevation Models (DEM) for topographic displacement.

The classification process was performed using the following bands: Blue, Green, Red, NIR, SWIR 1 and SWIR 2. Normalized indexes, such as NDVI (Normalized Difference Vegetation Index), NDWI (Normalized Difference Water Index) and NDBI (Normalized Difference Built-up Index) were also used in order to minimize the effects of topographic shading (SABOL JR. *et al.* 2002). Besides, those help to enhance the classification accuracy, by providing extra dimensions of separability.

Training areas for the defined land cover classes were selected in each image to identify bare soil areas, which were most representative of recent scars. The following land cover classes were defined: urban areas, bare soil, low vegetation (pasture and grasses), high vegetation (bushes and forests), and water.

According to Mather (2003), the minimum number of training areas per class for the specifications of this study (8 discriminant bands and 5 classes) must at least 48. In this sense, one hundred training areas were collected for each class. The Support Vector Machine (SVM) classifier was used

with the radial basis function kernel (SHAFRI & RAMLE, 2009) and a gamma value of 0.5. The penalty parameter was 500, and the classification probability threshold was 0.

To evaluate the accuracy of the resulting classification, validation samples, of 600 pixels for each class were collected adopting the stratified random sampling strategy (SMITS, DELLEPIANE & SCHOWENGERDT, 2010).

The results of the relief and land cover classification were analyzed together by the spatial intersection of the two datasets. Thus, bare soil areas located in regions of medium or high landslide susceptibility were considered potential landslide scars.

To evaluate the association of landslide scars and hazard areas with CNAAA access routes, a 500-meter analysis zone was defined around the access routes (GROWLEY, 2008). Each of the potential landslide areas was evaluated individually by means of visual interpretation, assessing the spectral behavior, shape and topography, according to Jaboyedoff et al. (2009), which identified the areas that corresponded to landslide scars and were identifiable on the LANDSAT 8 images.

3. Results

The results of the supervised land cover classification are presented in Figure 4. The classification result accuracy evaluation had a *kappa* index of 0.79 and 86.86% of overall accuracy. The confusion matrix and the commission and omission errors, presented in Table 2, show the detailed accuracy assessment, and it is possible to notice that main misclassification were among the Bare Soil and Urban Areas classes.

Table 2. Confusion Matrix and Commission and Omission Errors for the land cover classes.

	Urban Areas	High Vegetation	Water	Bare Soil	Low Vegetation	Total	Commission Error	Omission Error
Urban	74.82	0	2.55	19.92	0.75	11.1	17.86	25.18
High Vegetation	3.49	95.41	6.57	10.83	5.6	53.88	5.37	4.59
Water	0	4.15	75.2	0.19	0.12	13.51	16.63	24.8
Bare Soil	0.12	0	0.39	59.38	0.37	0.85	13.79	40.62
Low vegetation	21.57	0.44	15.29	9.67	93.15	20.65	46.8	6.85
Total	100	100	100	100	100	100	-	-

The high vegetation class is predominant in the study area. Bare soil occurs sparsely throughout the basin and in isolated areas. However, bare soil patches are also located in urban areas, especially in the northeast region of the basin. Small urban clusters and small patches of low vegetation are distributed along the coastline.

Figure 5 shows the landslide susceptibility map of the study area. Areas of high landslide susceptibility are distributed throughout the study area. In addition, the eastern portion of the study area contains a greater concentration of areas classified with low and medium

susceptibilities. A comparative analysis of the two maps shows that this region has the largest amount of human development the study area, which is likely because of the favorable terrain.

Table 3 shows the area (in hectares) and percentage of each land cover class and the landslide susceptibility level for the watershed and for the CNAAA access route zone.

In the watershed, most bare soil and urban areas (57% and 62.50%, respectively) are located in regions with average landslide susceptibility.

Table 3. Areas and percentages of land cover classes for the study watershed and for the access route zone by landslide susceptibility level.

	Class	Water		Low Vegetation		Bare soil		Urban Areas		High vegetation	
	Susceptibility	Area (ha)	%	Area (ha)	%	Area (ha)	%	Area (ha)	%	Area (ha)	%
Study Watershed	Low	1,350	18%	11,172	22%	660	37%	2,950	27%	50,915	18%
	Medium	4,310	56%	32,063	62%	1,106	62%	7,680	70%	135,314	46%
	High	1,991	26%	8,584	17%	22	1%	301	3%	105,366	36%
	Total	7,649	100%	51,819	100%	1,787	100%	10,930	100%	291,594	100%
Access Route Influence Zone	Low	309	24%	2,745	19%	207	35%	1,272	25%	3,656	17%
	Medium	936	71%	10,544	72%	385	64%	3,716	73%	12,481	56%
	High	65	5%	1,370	9%	6	1%	128	3%	5,954	27%
	Total	1,309	100%	14,659	100%	598	100%	5,116	100%	22,089	100%

The areas with high landslide susceptibility are mainly associated with the Serra do Mar escarpments because they have the most steeply sloping terrain. The predominant land cover class in these areas is high vegetation (36%), which corresponds to the Atlantic Forest. The class with the second highest percentage of high susceptibility area is water (26%), which is likely due to the confusion of the classifier because of shadows in areas of high vegetation. The class with the third highest percentage of high susceptibility area is low vegetation (17%), which is because it is more vulnerable to rainfall erosion and because it has less stable roots than the forest vegetation. These factors increase the instability of the slope and favor the occurrence of landslides (BIERMAN & MONTGOMERY, 2014).

The CNAAA access route zone has a similar pattern to that of the basin study area; 63.8% of the urban areas and 57% of the bare soils are located in areas of medium susceptibility. The same land cover pattern is observed at the highest susceptibility level.

The evaluation of bare soil areas in areas of medium or high landslide susceptibility identified 217.05 hectares of landslide scars, which corresponds to 53.77% of these susceptibility zones.

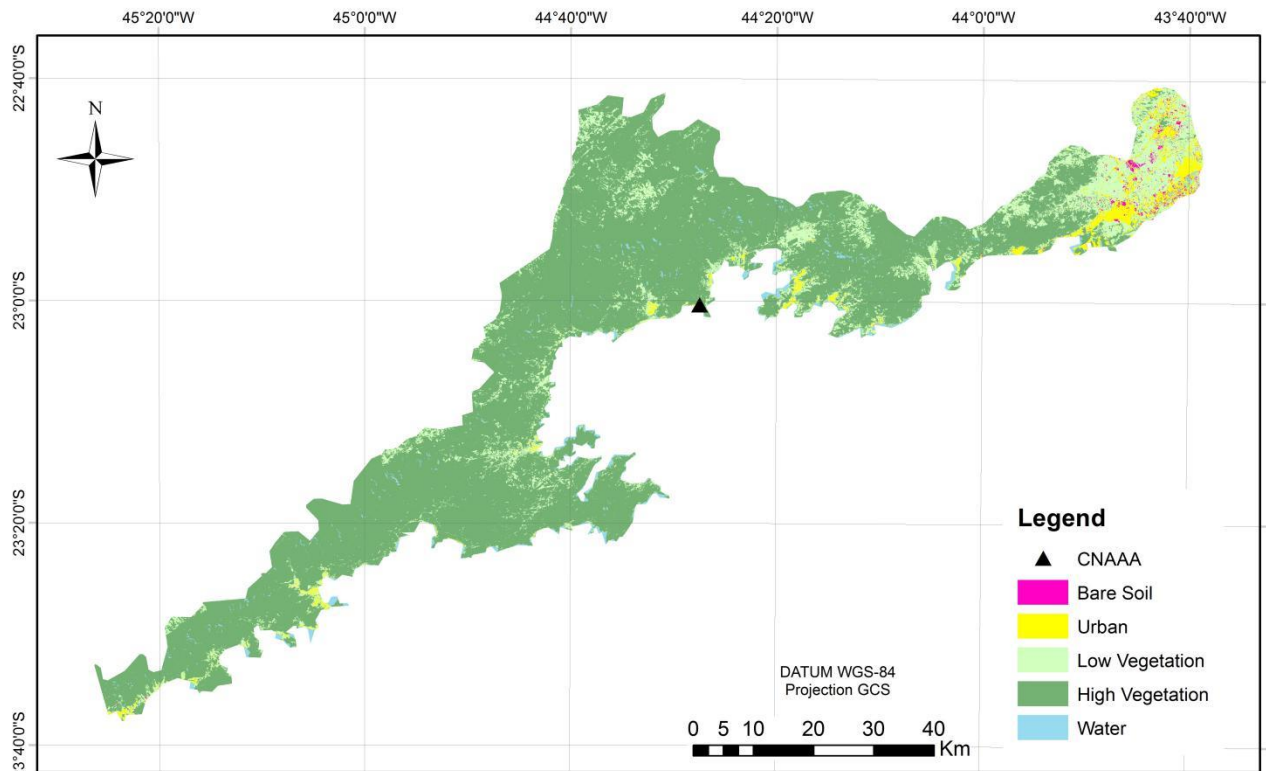


Figure 4. Map of the land cover in the study area based on LANDSAT 8 images from August and September, 2015.

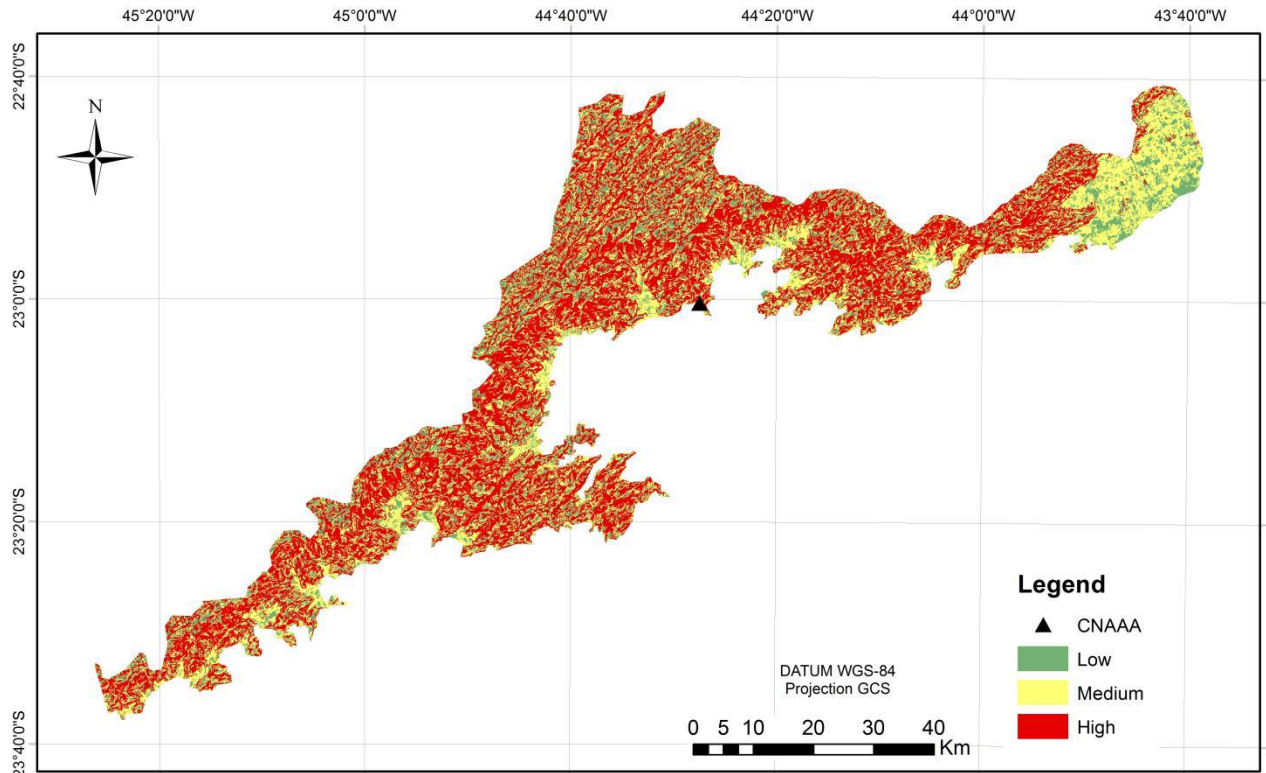


Figure 5. Map of landslides susceptibility of the study area based on TOPODATA data.

4. Discussion

The landslide susceptibility classification showed that the study area has high susceptibility along the whole watershed, exposing a critical situation for the landslide events occurrence. This characterization indicates that a detailed topographic inventory in a larger scale, around CNAAA, is paramount to define a preventive plan for the risk areas.

The land cover classification showed a *kappa* index of 0.79, which is a very good classification according to Landis and Koch (1977). However, several classification errors occurred, especially between the water classes and high vegetation. The classification errors are due to the existence of shadows in sloping areas, which alter the spectral responses of the targets. This factor results in changes in the statistics of the land cover classes by level of landslide susceptibility.

Confusion also occurred between the classifications of bare soil and urban area. According to Whitford, Ennos, and Handley (2001), classification errors between these two classes mainly occur due to roof tile materials, which produce a similar spectral behavior in urban areas and some types of bare soil.

When analyzing the map shown in Figure 5, it is important to highlight that the CNAAA is located in a region with many areas classified as high landslide susceptibility. The watershed generally contains only small regions of low landslide susceptibility. This information is demonstrated by the results shown in Table 3. In general, the results provide an important preliminary characterization of the landslide susceptibility and hazards in the watershed in which Brazil's only nuclear power plant is located.

According to Dias & Herrmann (2006) and Piedade *et al.* (2011), landslide susceptibility and hazard mapping requires detailed information about the soils, lithology and climate of the studied region. However, these data are often not available at a scale suitable for regional studies. Therefore, the presented methodology allows the preliminary regional evaluation to identify areas that should be analyzed in more detail.

The integrated assessment of the land cover map and the landslide susceptibility map provided important information about the pattern of occupancy and presence of hazard areas in the watershed since it is possible to identify urban areas in regions that are naturally susceptible to landslides. In addition, it revealed areas with the characteristics of scars from recent landslides (bare soil in areas with medium or high landslide susceptibility). This analysis provides an important characterization of the watershed and important indicators for preventive and mitigation actions in areas near the highways, especially considering the presence of a nuclear power plant in the region.

According to Smith (2013), hazard management for natural disasters and technological disasters must be integrated since technological disasters may be related to and triggered by natural disasters. Kobiyama *et al.* (2006) notes that preliminary mapping of landslide hazard areas and areas that are naturally susceptible to landslides facilitates hazard management and is key to preventing extreme events.

Considering the context of the CNAAA and the presence of few access and evacuation routes in the region, it is important that all hazard areas associated with highways be evaluated. Mitigation measures should be taken to maintain the integrity of roads that are essential for effective evacuation in the event of a technological disaster (RODRIGUES, 2014). In this way, both hazard

areas and the scars of landslides that have already occurred must be evaluated to guarantee road and traffic safety (GERMAN, ANDREY & KSENIA, 2015).

The potential landslide scars in the area surrounding the main access roads were evaluated individually through visual interpretation of satellite images, and 53.77% of the area was evaluated as landslide scars. This percentage demonstrates the great potential of the procedures for identifying scars over large areas using satellite images since they reduce the area to be interpreted visually by the analyst and indicate candidate areas with greater potential of landslide occurrence. The features identified as “non-scars” are mainly due to errors in land cover classification (confusion between bare soil and urban areas).

However, it is important to highlight that the exclusive use of the bare soil cover class restricts the landslide scars to those that occurred recently and excludes older scars that have already been covered by low vegetation. This evolution in land cover was noted by Walker Shields (2013), Walker and Del Moral (2003), and Joshi (1990) and complicates the process of identifying scars by remote sensing.

It is important to emphasize that the procedures and results presented in this study do not eliminate the need for fieldwork for an effective evaluation. However, the results highlight the main areas that require more detailed surveys based on variables such as the soil type and geology (ANDRETTA *et al.*, 2013).

Traffic in the study area can also be interrupted by road safety issues, such as bad signaling, lack of road maintenance, and possible road drainage problems (MAZZETTO, 2015). Road safety assessments and simulations are important for managing the risk of technological disasters and ensuring the effectiveness of evacuation plans (LUCAS *et al.*, 2013).

In addition, it is important to carry out simulations of interruptions of access roads in the regions at greatest risk of landslides that would affect the roads to establish alternative evacuation plans for the CNAAA. However, to simulate the interruption of the road flow and design alternative routes, it is necessary to complement the road network by digitizing small roads that are not on the official maps, which would increase the value of the analysis and ensure the development of more efficient evacuation plans for the CNAAA.

5. Conclusion

This study provided a primary synthesis of the landslides risk on CNAAA watershed and on buffer of the access roads. The majority of the study area is medium or high risk for landslide events, representing a risk to execute the evacuation of the affected area in a technological disaster event. Besides, the potential of landslides scars mapping was assessed, achieving over 50% of accuracy. This is presented as a potential methodology for the risk assessment and landslides monitoring in the study area, in order to maintain the access roads available for eventual evacuations.

The Admiral Álvaro Alberto Nuclear Power Plant in the city of Angra dos Reis, RJ, is an area of focus due to the potential for technological accidents, and it is located in a region with many historic landslides, which were generally associated with high intensity rainfall events. The presence of highways in these regions, which are naturally susceptible to landslides, may increase the likelihood of landslides. Therefore, mapping and identifying hazard areas and landslide scars have

become important for the prevention and mitigation of extreme events, maintaining the integrity of the access routes and designing emergency evacuation strategies.

However, mapping and monitoring these areas are not trivial tasks because highways cross large areas, and the limited accessibility of the region make *in situ* assessments difficult. Therefore, remote sensing and geoprocessing techniques can be used as mapping tools.

This study mapped areas susceptible to the occurrence of landslides by classifying relief features based on TOPODATA slope and vertical and horizontal curvature data. It used an object-based approach that yielded classes of low, medium, and high landslide susceptibility. In addition, this study identified landslide scars through land cover classification from LANDSAT images and the SVM supervised classification algorithm. Bare soil areas were considered most representative of recent scars. The results of this mapping procedure were evaluated through the *kappa* index and the confusion matrix.

The integrated assessment of the land cover map and the landslide susceptibility map provided important information about the pattern of occupancy and the presence of hazard areas in the watershed, which allowed the identification of urban areas in landslide-susceptible areas. Despite being performed on a regional scale, the procedure allowed the identification of areas of the highest landslide susceptibility, which helped to select areas that require more detailed analyses.

The procedures can easily be replicated by public agencies responsible for monitoring hazard areas because free data were used, and the results provided satisfactory identification of the areas most susceptible to landslides. Although, the results should be considered tentative at this stage, and further research is required to verify these preliminary findings and replicate them to a broader area.

ACKNOWLEDGEMENT

The authors acknowledge the research scholarship provided by CNPq, to the Escola Politécnica da Universidade de São Paulo and Laboratório de Geoprocessamento do Departamento de Engenharia de Transportes da EPUSP.

REFERENCES

- Aksoy, B.; Ercanoglu, M. 2012. Landslide identification and classification by object-based image analysis and fuzzy logic: An example from the Azdavay region (Kastamonu, Turkey). *Computers & Geosciences*, v. 38, n.1, p. 87-98.
- Alexakis, D.D.; Agapiou, A.; Tzouvaras, M.; Themistocleous, K.; Neocleous, K.; Michaelides, S.; Hadjimitsis, D.G. 2014. Integrated use of GIS and remote sensing for monitoring landslides in transportation pavements: the case study of Paphos area in Cyprus. *Natural Hazards*, v. 72, n. 1, p. 119-141.
- Andretta, E.R.; Ladeira, L.F.B.; Santos, J.M.; Lima, R.H.C. 2013. Mapeamento das Áreas de Risco no Bairro Gilberto Mestrinho, Zona leste de Manaus–AM. *Estudos Geológicos*, v. 23, n. 1, p. 3-11.
- Araújo, D. & Oliveira, R. 1988. Reserva Biológica Estadual da Praia do Sul (Ilha Grande, Estado do Rio de Janeiro): Lista preliminar de flora. *Acta Botânica Brasileira*, n. 1, p. 83-94.

- Azevedo, G.F. 2016. *Sistema de análise quantitativa de risco por escorregamentos rasos deflagrados por chuvas em regiões tropicais*. Tese (Doutorado) – Universidade de Brasília, Brasília.
- Barlow, J.; Martin, Y.; Franklin, S.E. 2003. Detecting translational landslide scars using segmentation of Landsat ETM+ and DEM data in the northern Cascade Mountains, British Columbia. *Canadian Journal of Remote Sensing*, v. 29, n. 4, p. 510-517.
- Bierman, P. R. and Montgomery, D. R. 2014. Hillslope. In: *Key Concepts in Geomorphology*. W. H. Freeman and Company Publishers New York, pp. 145-178.
- Camargo, F. F.; Almeida, C. M.; Florenzano, T. G.; Heipke, C.; Feitosa, R. Q.; Costa, G. A. O. P. 2012. ASTER/Terra imagery and a multilevel semantic network for semi-automated classification of landforms in a subtropical area. *Photogrammetric Engineering & Remote Sensing*, v. 77, n. 6, p. 619-629.
- Christofolletti, A. 1980. *Geomorfologia*. 2 ed. São Paulo: Edgard Blücher, 1980.
- CPRM - Companhia de Pesquisa de recursos minerais/serviço geológico do Brasil. 2007. *Programa Geologia do Brasil: Geologia da Folha Angra dos Reis*. Disponível em: <http://www.cprm.gov.br/publique/media/rel_angra.pdf, 2007>. Acesso em: nov. 2016.
- Dai, F.C.; Lee, C.F. 2001. Frequency–volume relation and prediction of rainfall-induced landslides. *Engineernig Geology*, v. 59, p. 253–266.
- De Vita, P.; Napolitano, E.; Godt, J.W.; Baum, R.L. 2013. Deterministic estimation of hydrological thresholds for shallow landslide initiation and slope stability models: case study from the Somma-Vesuvius area of southern Italy. *Landslides*, v.10, n. 6, p. 713-728.
- Di Martino, L.; Masciocco, L.; Ricca, G.; Toja, M. 2014. Relationships between landslides phenomena and road network: An example from hilly region of Asti Province (North-Western Italy). *Engineering Geology for Society and Territory*, v. 2, p. 1049-105.
- Dias, F. P.; Herrmann, M. L. de P. 2006. Susceptibilidade a deslizamentos: estudo de caso no bairro Saco Grande, Florianópolis–SC. *Caminhos de Geografia*, v. 3, n. 6, p.57-73.
- Doleire-Oltmanns, S.; Eisank, C.; Dragut, L.; Blaschke, T. 2013. An object-based workflow to extract landforms at multiple scales from two distinct data types. *IEEE Geoscience and Remote Sensing Letters*, v. 10, n. 4, p. 947-951.
- Dong, J.; Lai, P.; Chang, C.; Yang, S.; Yeh, K.; Liao, J.; Pan, Y. 2014. Deriving landslide dam geometry from remote sensing images for the rapid assessment of critical parameters related to dam-breach hazards. *Landslides*, v.11, n. 1, p. 93-105.
- Drăguț, L.; Eisank, C. 2012. Automated object-based classification of topography from SRTM data. *Geomorphology*, v. 141, p. 21-33.
- Eisank, C.; Drăguț, L.; Blaschke, T. 2011. A generic procedure for semantics-oriented landform classification using object-based image analysis. *Geomorphometry*, p. 125-128.
- Fernandes, N. F.; Amaral, C. P. 1996. Movimentos de massa: uma abordagem geológico-geomorfológica. In: GUERRA A.J.T.; CUNHA, S. (Org.). *Geomorfologia e meio ambiente*. 1 ed. Rio de Janeiro: Bertrand Brasil, cap. 3. p. 123-194.
- Florenzano, T.G. 2016. *Geomorfologia: conceitos e tecnologias atuais*. Oficina de Textos.

- German, Postoev; Andrey, Kazeev; Ksenia, Fedotova. 2015. About the Landslide Hazard Criteria for the Transportation Safety of the 2014 Sochi Olympics. In: *Engineering Geology for Society and Territory-Volume 2*. Springer International Publishing, p.1469-1472.
- Growley, B. 2008. Landslide Susceptibility Zonation GIS for the 2005 Kashmir Earthquake affected region. Dissertação (Mestrado) – University of Montana.
- Guzzetti, F.; Mondini, A. C. Cardinali, M.; Fiorucci, F.; Santangelo, M.; Chang, K-T. 2012. Landslide inventory maps: new tools for an old problem. *Earth Science Reviews*, v. 112, p. 42-66.
- Hsieh, Y.; Hou, C.; Chan, Y.; Hu, J.; Fei, L.; Chen, H.; Chiu, C. 2014. Detection and Volume Estimation of Large Landslides by Using Multi-temporal Remote Sensing Data. *EGU General Assembly Conference Abstracts*. v.16, p. 5725.
- IPT – Instituto de pesquisas tecnológicas do Estado de São Paulo S.A. 1991. *Ocupação de encostas*. Coord. de Cunha, M.A. São Paulo: Instituto de Pesquisas Tecnológicas, – Publicação IPT n.1831.
- IPT – Instituto de pesquisas tecnológicas do Estado de São Paulo S.A. 2002. *Assessoria Técnica para a Estabilização de Encostas, Recuperação da Infra-estrutura Urbana e Reurbanização das Áreas de Risco Atingidas por Escorregamentos na Área Urbana do Município de Campos do Jordão, SP*. Relatório Técnico 64.399, São Paulo.
- Jaboyedoff, M.; Demers, D.; Locat, J.; Locat, A.; Locat, P.; Oppikofer, Robitaille, D.; Turmel, D. 2009. Use of terrestrial laser scanning for the characterization of retrogressive landslides in sensitive clay and rotational landslides in river banks. *Canadian Geotechnical Journal*, v. 46, n. 12, p. 1379-1390.
- Jaiswal, P.; Van Westen, C. J.; Jetten, V. 2011. Quantitative assessment of landslide hazard along transportation lines using historical records. *Landslides*, v. 8, n. 3, p. 279-291.
- Joshi, M. 1990. A study on Soil and Vegetation Changes after landslide in Kumaun Himalaya. *Proceedings of the Indian National Science Academy.*, n. 4, p. 351-360.
- Kobiyama, M.; Mendonça, M.; Moreno, D. A.; Marcelino, I.; Marcelino, E.; Gonçalves, E.; Brazetti, L.; Goerl, R.; Moller, G.; Rudorff, F. 2006. *Prevenção de desastres naturais: conceitos básicos*. Curitiba: Organic Trading.
- Landis, J.R.; Koch, G.G. 1977. The measurement of observer agreement for categorical data, *Biometrics*, p. 159-174.
- Lange Filho, G. 2016. *Caracterização e mapeamento dos modelados padrões e formas de relevo simbolizadas da bacia hidrográfica do Ribeirão Itoupava, Blumenau-SC*. Dissertação (Mestrado) – Universidade Federal do Paraná, Curitiba.
- Larsen, M.C.; Parks, J.E. 1997. How wide is a road? The association of roads and mass-wasting in a forested montane environment. *Earth Surface Processes and Landforms*, v. 22, n. 9, p. 835-848.
- Lousada, G.; Farias, H. 2015. Desastres Ambientais, Prevenção e Mitigação: Um Estudo de Caso da Região de Angra dos Reis/RJ. *Revista Continentes*, v. 3, n. 5, p. 131-149.
- Lucas, F.R.; Russo, L.E.A.; Kawashima, R.S.; Figueira, A.C.; Larocca, A.P.C.; Kabbach JR.; F.I. 2013. Uso de simuladores de direção aplicado ao projeto de segurança viária. *Boletim de Ciências Geodésicas*, v. 19, n. 2, p.341-352.
- Manconi, A.; Casu, F.; Ardizzone, F.; Bonano, M.; Cardinali, M.; DE Luca, C.; Gueguen, E.; Marchesini, I.; Parise, M.; Vennari, C.; Lanari R.; Guzzetti, F. 2014. BRIEF Communication: Rapid

mapping of landslide events: the 3 December 2013 Montescaglioso landslide, Italy. *Natural Hazards and Earth System Science*, v. 14, n. 7, p. 1835-1841.

Manfré, L.A.; Nóbrega, R.A.A.N.; Quintanilha, J.A. 2014. Regional and local topography subdivision and landform mapping using SRTM-derived data: a case study in southeastern Brazil. *Environmental Earth Sciences*, v. Online, p.1-19.

Mather, P.M. 2003. *Geoenvironmental mapping: methods, theory and practice*. Victoria, Canada: Sage Publications, 143 p..

Mazzetto, L.F. 2015. *Avaliação das condições de segurança em rodovias federais da região metropolitana de Curitiba*. Universidade Federal Tecnológica do Paraná, Curitiba. Monografia (Especialização) – Universidade Tecnológica Federal do Paraná, Curitiba.

Mckean, J.; Buechel, S.; Gaydos, L. 1991. Remote sensing and landslide hazard assessment. *Photogrammetric Engineering & Remote Sensing*, v. 57, n. 9, p.1185-1193.

Paulín, G. L.; Hubp, J. L.; Quesada, J. F. A. 2014. Assessing Landslide Frequency for Landform Hazard Zoning Purposes. In: Sassa, K.; Canuti, P.; Yin, Y. *Landslide Science for a Safer Geoenvironment*. Netherlands: Springer, v. 2, p. 129-134.

Penna, D.; Borga, M.; Aronica, G. T.; Brigandì, G.; Tarolli, P. 2013. Predictive power of a shallow landslide model in a high resolution landscape: dissecting the effects of forest roads. *Hydrology and Earth System Sciences Discussions*, v. 10, n. 7, p. 9761-9798.

Pinheiro, J.C.; Aguiar, P.R.R. 2015. Impacto da Construção da Base de Submarinos na Economia de Itaguaí-RJ. *UNOPAR Científica Ciências Exatas e Tecnológicas*, v. 11, n. 1, p.31-40.

Pradhan, B.; Lee, S. 2010. Delineation of landslide hazard areas on Penang Island, Malaysia, by using frequency ratio, logistic regression, and artificial neural network models. *Environmental Earth Sciences*, v. 60, n. 5, p.1037-1054.

Rodrigues, A.S. 2014. *Método para elaboração de um plano de evacuação emergencial em uma usina nuclear utilizando microssimulação de tráfego*. Dissertação (Mestrado em Engenharia Civil) – Universidade Federal de Santa Catarina, Florianópolis.

Roessner, S.; Behling, R.; Segl, K.; Golovko, D.; Wetzel, H.; Kaufmann, H. 2014. Automated Remote Sensing Based Landslide Detection for Dynamic Landslide Inventories. In: Sassa, K.; Canuti, P.; Yin, Y. *Landslide Science for a Safer Geoenvironment*. Netherlands: Springer, v. 2, p.345-350.

Sabol JR., D.E.; Gillespie, A.R.; Adams, J.B.; Smith, M.O.; Tucker, C.J. 2002. Structural stage in Pacific Northwest forest estimated using mixing models of multispectral images. *Remote Sensing of Environment*, v. 80, n. 1, p. 1-16.

Sestini, M. F. 1999. *Variáveis geomorfológico no estudo de escorregamentos em Caraguatatuba-SP utilizando imagens TM-LANDSAT e SIG*. Dissertação (Mestrado em Sensoriamento Remoto) – Instituto Nacional de Pesquisas Espaciais – INPE, São José dos Campos.

Shafri, H.Z.M.; Ramle, F.S.H. 2009. A Comparison of Support Vector Machine and Decision Tree Classifications Using Satellite Data of Langkawi Island. *Information Technology Journal*, v. 8, n. 1, p. 64-70.

Silva Junior, C.H.L.; Silva, F.B.; Pereira, D.C.A. 2016. Uso de lógica fuzzy e processo analítico hierárquico–ahp no zoneamento de áreas suscetíveis a deslizamento utilizando o operador fuzzy média ponderada ahp o caso da bacia hidrográfica do Rio Anil em São Luís–MA. *Revista de Geografia-PPGEO-UFJF*, v. 3, n. 2, p. 1-7.

- Smith, K. 2013. *Environmental hazards: assessing risk and reducing disaster*. Routledge.
- Smits, P.C.; Dellepiane, S.G.; Schowengerdt, R.A. 2010. Quality assessment of image classification algorithms for land-cover mapping: A review and a proposal for a cost-based approach. *International Journal of Remote Sensing*, v. 20, n. 8, p. 1461-1486.
- Tarolli, P.; Calligaro, S.; Cazorzi, F.; Dalla Fontana, G. 2013. Recognition of surface flow processes influenced by roads and trails in mountain areas using high-resolution topography. *European Journal of Remote Sensing*, v. 46, p.176-197.
- Piedade, A.; Zêzere, J. L; Garcia, R.; Oliveira, S. 2011. Modelos de susceptibilidade a deslizamentos superficiais translacionais na região a norte de Lisboa. *Finisterra*, v. 46, n. 91.
- Valeriano, M.M.; Rossetti, D.F. 2012. Topodata: Brazilian full coverage refinement of SRTM data. *Applied Geography*, v. 32, n. 2.
- Vieira, B. C. 2007. *Previsão de escorregamentos translacionais rasos na Serra do Mar (SP) a partir de modelos matemáticos em bases físicas*. Tese (Doutorado em Geografia) – Instituto de Geociências, Universidade Federal do Rio de Janeiro, Rio de Janeiro.
- Walker, L.R.; Del Moral, R. 2003. *Primary Sucession and Ecosystem Rehabilitation*. Cambrige University Press, Reino Unido.
- Walker, L.R.; Shiels, A.B. 2013. *Landslide Ecology*. Cambridge University Press, 1ª Edição, New York, 300 p.
- Whitford, V.; Ennos, A. R.; Handley, J. F. 2001. City form and natural process—indicators for the ecological performance of urban areas and their application to Merseyside, UK. *Landscape and urban planning*, v. 57, n. 2, p. 91-103.